Preprints of the 21st IFAC World Congress (Virtual)
Berlin, Germany, July 12-17, 2020

Simultaneous Active and Reactive Power Sharing with Frequency Restoration and Voltage Regulation for Single Phase Microgrids

Miguel Parada Contzen *

* *Electric and Electronics Engineering Department, Universidad del Bío-Bío, Chile (e-mail: mparada@ubiobio.cl).*

Abstract: The control of microgrids at secondary hierarchical level offers multiple challenges. When the entire microgrid is seen as a Multiple-Input-Multiple-Output (MIMO) system and the Voltage Source Inverters (VSI) connected as control actuators, distributed controllers have been proposed to independently achieve active power sharing, reactive power sharing, frequency restoration, or voltage regulation around nominal values. Here we address these issues simultaneously in generic single phase mesh-micro-grids with arbitrary non-linear loads, in order to derive formal conditions that can be used to check if a given controller allows to reach all four mentioned control objectives. The paper is complemented with a simulation example where the main characteristics of the proposed methodology can be seen.

Keywords: Agents, Distributed control, Microgrids, Power-system control, Reactive power, Active power, Synchronization, Voltage regulation

1. INTRODUCTION

At the secondary level of the hierarchical control scheme typically used for microgrids, see for example (Guerrero et al., 2013; Palizban and Kauhaniemi, 2015; Bidram and Davoudi, 2012), several control objectives are proposed. For three phase AC microgrids, active and reactive power sharing (Han et al., 2016) are the most relevant, and several publication deal with the topic independently for the active and reactive cases, *e.g* (Schiffer et al., 2014; Lu and Chu, 2015; Parada Contzen and Raisch, 2016).

In order to achieve power sharing, the frequency and voltage amplitude of the controlled voltage source inverters (VSI) need to be modified from its nominal value. Therefore, nominal frequency restoration and voltage regulation strategies are also considered as secondary level control objectives. Some publications that deal with this aspects are (Parada Contzen, 2019; Guo et al., 2015; Simpson-Porco et al., 2013, 2015). More recently, these secondary control issues have been addressed by books as (Zambroni de Souza and Castilla, 2019; Guo et al., 2018).

Based on the quoted publications, in this paper we focus on single phase AC microgrids and the simultaneous achievement of the four described secondary level control objectives. Exploding the similarities between single- and three-phase power models, in the following Section we propose a linearized model of the microgrid, valid when it is desired to operate around a nominal point given by RMS voltage and frequency. Based on this model, Section 3 formally define the four control objectives and propose a distributed control strategy, whose performance can be easily evaluated through standard control theoretical tools and demand little communication requirements. As far as the author knows, a formal stability analysis including all four control objectives simultaneously has not been addressed before, and the proposed procedure is general enough to admit several variations on models or control objectives. Finally, Section 4 illustrates the closed loop analysis with help of a simulation example.

Through this paper, matrix $\boldsymbol{A}'$ is the transpose of $\boldsymbol{A}$. The identity matrix and the null matrix are respectively denoted by $\boldsymbol{I}$ and $\boldsymbol{0}$. A column vector of ones is denoted as $\boldsymbol{1}$, and a vector with zeros in every position except in the i-th row where its value is one, is denoted as $\boldsymbol{s}_i \in \mathbb{R}^N$ so that $\sum_{i=1}^{N} \boldsymbol{s}_i = \boldsymbol{1}$. If necessary, the dimensions of these matrices will be stated as an index. An element in position (i, j) of a matrix $\boldsymbol{A}$ is denoted $[\boldsymbol{A}]_{ij}$.

2. MICROGRID MODEL

2.1 Model and control of a voltage source inverter (VSI)

The model proposed in this section is based on the internal control strategies described in, *e.g.*, Peças Lopes et al. (2006); Rocabert et al. (2012); Schiffer et al. (2016). As one can consider that a multi-phase power electronic devices is a collection of single-phase circuits, the models in this section are fundamentally the same as the three-phase models that can be found in Parada Contzen (2019); Parada Contzen and Raisch (2016) and the references within.

The single-phase voltage output of a Voltage Source Inverter (VSI) can be described by its amplitude $V_i(t) = V(1 + \nu_i(t)) > 0$ and its electric angle $\psi_i(t) := \omega t + \delta_i(t)$, where $\nu_i(t) \in \mathbb{R}$ is the deviation in per unit of the RMS value $V \in \mathbb{R}$, $\omega = 2\pi f > 0$ is a constant nominal angular

Copyright lies with the authors

frequency, with $f > 0$ the nominal frequency in Hertz, and $\delta_i(t) \in \mathbb{R}$ is the phase shift angle with respect to a fixed arbitrary reference. The variation of the voltage amplitude around its nominal value is normed according to local and regional regulations with a realistic bound $|\nu_i(t)| < 5.0\% \ll 1$.

The intern dynamics of the inverters can be considered very fast, and therefore they are typically neglected. In this case, the input/output relationships for the operation (angular) frequency $\omega_{o,i} := \dot{\psi}_i(t)$ and the voltage amplitude $V_i(t)$ at node $i \in \mathcal{V}$, considering internal control loops, switching modulation and appropriate filtering, can be modeled as in (Schiffer et al., 2014, 2016, etc.) with the following equations:

$$\begin{aligned} \dot{\psi}_i(t) &= d^{\psi_i}(t), \\ V_i(t) &= d^{V_i}(t), \end{aligned} \tag{1}$$

where $d^{\psi_i}(t) \in \mathbb{R}$ and $d^{V_i}(t) \in \mathbb{R}$ are, respectively, the frequency and amplitude control inputs. This model assumes that each inverter is equipped with some DC storage unit, large enough to increase and decrease the AC power output in a certain range.

When the inverter is operated around the nominal frequency ω and RMS value V, the inputs can be modified as $d^{\psi_i}(t) = \omega + \kappa u_i^{\psi}(t)$ and $d^{V_i}(t) = V(1 + u_i^V(t))$, where $u_i^{\psi}(t)$ and $u_i^V(t)$ are inputs that control small variations of the original signals around the nominal values. The term $\kappa > 0$ is a constant thought to limit the magnitude of the frequency input after feedback.

With this, the intern dynamics of inverter i in (1) can be written as:

$$\begin{aligned} \dot{\delta}_i(t) &= \kappa u_i^{\psi}(t), \\ \nu_i(t) &= u_i^V(t). \end{aligned} \tag{2}$$

Additionally, we are interested on the frequency deviation with respect to nominal frequency $\upsilon_i(t) := \dot{\psi}_i(t) - \omega = \dot{\delta}_i(t)$. Deriving equation (2), we can model the dynamics of the frequency deviation by the following expression

$$\dot{\upsilon}_i(t) = \kappa \dot{u}_i(t). \tag{3}$$

We assume that $\upsilon_i(t)$ cannot be directly measured and used for feedback.

From here, a the set of inverters can be characterized as a network of agents with two control inputs described by the following compact equations:

$$\begin{aligned} \boldsymbol{\upsilon} &:= \dot{\boldsymbol{\delta}} = \kappa \boldsymbol{u}^{\psi}, \\ \boldsymbol{\nu} &:= \boldsymbol{u}^V, \end{aligned} \tag{4}$$

where $\boldsymbol{\delta} = \operatorname{col}\{\delta_i(t)\}_{i\in\mathcal{V}}$, $\boldsymbol{\nu} = \operatorname{col}\{\nu_i(t)\}_{i\in\mathcal{V}}$, $\boldsymbol{u}^V := \operatorname{col}\{u_i^V(t)\}_{i\in\mathcal{V}}$, and $\boldsymbol{u}^{\psi} := \operatorname{col}\left\{u_i^{\psi}(t)\right\}_{i\in\mathcal{V}}$. Note that $\dot{\boldsymbol{\upsilon}} = \kappa \dot{\boldsymbol{u}}$ and the mean value of the amplitude deviation is given by $\bar{\nu} = \frac{1}{N}\mathbf{1}'\boldsymbol{\nu}$.

2.2 Circuital model of the grid

An electric grid can be described as an undirected graph $\mathcal{C} = (\mathcal{V}, \mathcal{E})$, where the vertices are a collection of N electric nodes $i \in \mathcal{V}$ where the single-phase generation units studied in Subsection 2.1 are connected. These sources can be considered control actuators for the electric transmission process. The undirected edges of the graph are transmission lines between the nodes, denoted $(i, j) \in \mathcal{E}$. Any passive circuit can be equivalently represented by this structure through a Kron reduction procedure as described in (Dörfler and Bullo, 2013; Grainger and Stevenson, 1994).

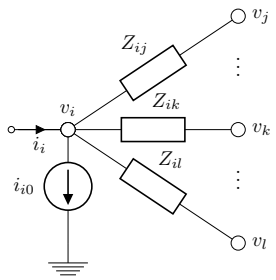

Fig. 1. Voltage and current at node $i \in \mathcal{V}$ of a Single phase AC microgrid with $\mathcal{N}_i = \{j, ..., k, ..., l\}$.

At every active node $i \in \mathcal{V}$, we will consider a load described by an arbitrary time variant sinusoidal current source. A transmission line $(i, j) \in \mathcal{E}$ between nodes i and $j \neq i$ will be assumed as an impedance composed by a resistance R_{ij} in series with an inductance L_{ij}. It is assumed that these line parameters are constant and can be estimated with reasonable accuracy.

Consider the circuit depicted in Figure 1, where the i-th node is shown. The voltage induced by the voltage source can be denoted as $v_i(t) = \sqrt{2}V_i(t)\sin(\psi_i(t))$, $\forall i \in \mathcal{V}$. The load is described by a current source consuming a sinusoidal current $i_{i0}(t)$ and the resulting current injected by the source is denoted as $i_i(t)$. An expression for this current can be obtained from a circuital analysis of the grid. From here, when $\psi_i(t) = \omega t + \delta_i(t)$, neglecting the transient behavior of the line dynamics, the active and reactive power injected by each source can be modeled by expressions that, for all generation units $i \in \mathcal{V}$, are quadratic in the voltage RMS value, $V_i(t)$, and trigonometric in the phase angle, $\delta_i(t)$, with respect to a fixed reference. For simplicity, from here on we will drop the explicit time dependence of the variables.

When the voltage amplitudes are bounded around its nominal value, *i.e.* when $V_i(t) = V(1 + \nu_i(t)) \approx V \iff \nu_i(t) \approx 0$, and the phase angles of the different voltages are small, *i.e.* $\delta_i(t) \approx \delta_j(t) \iff \theta_{ij}(t) := \delta_i(t) - \delta_j(t) \approx 0$, then a linearized model can be stated around the described operation point. Indeed, defining

$$P_{ij} = \frac{R_{ij}}{R_{ij}^2 + \omega^2 L_{ij}^2} V^2, \;\; Q_{ij} = \frac{\omega L_{ij}}{R_{ij}^2 + \omega^2 L_{ij}^2} V^2,$$

the expressions for active and reactive power can be simplified by a Taylor linearization in the following way:

$$\begin{aligned} P_i(t) = P_{i0} &+ \sum_{j\in\mathcal{N}_i} P_{ij}(1+\nu_i)^2 \\ &- \sum_{j\in\mathcal{N}_i} P_{ij}(1+\nu_i)(1+\nu_j)\cos(\theta_{ij}) \\ &+ \sum_{j\in\mathcal{N}_i} Q_{ij}(1+\nu_i)(1+\nu_j)\sin(\theta_{ij}) \\ \approx P_{i0} &+ \sum_{j\in\mathcal{N}_i} P_{ij}(\nu_i - \nu_j) + \sum_{j\in\mathcal{N}_i} Q_{ij}\theta_{ij}. \end{aligned}$$

$$
\begin{aligned}
Q_i(t) = Q_{i0} &+ \sum_{j\in\mathcal{N}_i} Q_{ij}(1+\nu_i)^2 \\
&- \sum_{j\in\mathcal{N}_i} Q_{ij}(1+\nu_i)(1+\nu_j)\cos(\theta_{ij}) \\
&- \sum_{j\in\mathcal{N}_i} P_{ij}(1+\nu_i)(1+\nu_j)\sin(\theta_{ij}) \\
\approx Q_{i0} &+ \sum_{j\in\mathcal{N}_i} Q_{ij}(\nu_i-\nu_j) - \sum_{j\in\mathcal{N}_i} P_{ij}\theta_{ij}.
\end{aligned}
$$

This approximation can be generalized to all nodes $i \in \mathcal{V}$ of the microgrid as in the following equation:

$$
\begin{bmatrix} \boldsymbol{p} \\ \boldsymbol{q} \end{bmatrix} = \begin{bmatrix} \boldsymbol{p}_0 \\ \boldsymbol{q}_0 \end{bmatrix} + \begin{bmatrix} \boldsymbol{C}_Q & \boldsymbol{C}_P \\ -\boldsymbol{C}_P & \boldsymbol{C}_Q \end{bmatrix} \begin{bmatrix} \boldsymbol{\delta} \\ \boldsymbol{\nu} \end{bmatrix}, \tag{5}
$$

where the power injected by at the nodes is given by $\boldsymbol{p} = \operatorname{col}\{P_i(t)\}_{i\in\mathcal{V}}$ and $\boldsymbol{q} = \operatorname{col}\{Q_i(t)\}_{i\in\mathcal{V}}$, the power consumed by the loads is given by $\boldsymbol{p}_0 = \operatorname{col}\{P_{i0}(t)\}_{i\in\mathcal{V}}$ and $\boldsymbol{q}_0 = \operatorname{col}\{Q_{i0}(t)\}_{i\in\mathcal{V}}$, and the matrices that describe the distribution circuit are such that

$$
[\boldsymbol{C}_Q]_{ij} = \begin{cases} \sum_{k\in\mathcal{N}_i} Q_{ik} & \text{, if } i = j \\ -Q_{ij} & \text{, if } i \neq j \in \mathcal{N}_i \\ 0 & \text{, in other case} \end{cases}
$$

and

$$
[\boldsymbol{C}_P]_{ij} = \begin{cases} \sum_{k\in\mathcal{N}_i} P_{ik} & \text{, if } i = j \\ -P_{ij} & \text{, if } i \neq j \in \mathcal{N}_i \\ 0 & \text{, in other case} \end{cases}
$$

Note that with these definitions, matrices $\boldsymbol{C}_p = \hat{L}(\mathcal{C}_p)$ and $\boldsymbol{C}_q = \hat{L}(\mathcal{C}_q)$ coincide with the Laplacian matrices of weighted graphs with the same edges that the microgrid and weights given by respectively P_{ij} and Q_{ij}.

Equation (5) represents a linearized model of the grid. For a discussion on the influence of the non-linearities see, for example, Parada Contzen (2019), where very similar models are used separately for the case of active power in three-phase grids. Note however, that any Lyapunov stability related condition obtained from approximation (5) is a necessary condition for global stability of the non-linear model.

In the quoted publications, when active and reactive power are studied independently, the model used is a special case of (5) that considers either $\boldsymbol{\nu} = \boldsymbol{0}$ for active power or $\boldsymbol{\delta} = \boldsymbol{0}$ for reactive power. Therefore, matrix $\boldsymbol{C}_P$ is not presented in the models already analyzed. Here, however, this matrix describe the crossed influence of the independent variables $\boldsymbol{\delta}$ and $\boldsymbol{\nu}$ over reactive and active powers.

Instead of dealing directly with the injected powers at node $i \in \mathcal{V}$ measured in $[kW]$ or $[kVA]$, it is usual to treat power as a dimensionless quantity $\bar{P}_i = P_i/\chi_i$ or $\bar{Q}_i = Q_i/\chi_i$ measured in per unit $[p.u.]$. That is, relative to a base quantity $\chi_i > 0$. A practical choice of the proportional constants would be the nominal power rating S_i of the respective generation unit. Also, different bases could be considered for Active and Reactive power, although we use the same one for simplicity. By defining $\boldsymbol{F} = \operatorname{diag}\{\chi_i\}_{i\in\mathcal{V}}$, we can define $\bar{\boldsymbol{p}} = \boldsymbol{F}\boldsymbol{p}$ and $\bar{\boldsymbol{q}} = \boldsymbol{F}\boldsymbol{q}$. It is also useful to define the per unit change rate of the loads as $\bar{\boldsymbol{w}}_p = \dot{\bar{\boldsymbol{p}}}$ and $\bar{\boldsymbol{w}}_q = \dot{\bar{\boldsymbol{q}}}$.

3. CLOSED LOOP ANALYSIS

3.1 Control Objectives

We are interested in four different control objective. First, Active and Reactive power sharing can be treated as consensus problems like in the quoted publications. Beside these two objectives, we are also interested in synchronization of the grid at nominal frequency and voltage amplitude regulation, *i.e.* in limiting the deviation of the amplitudes with respect to the nominal value.

For power sharing, we will define the following linear transformation:

$$
\boldsymbol{T} = D'(\mathcal{T}^o) = [\boldsymbol{1}_{N-1} \ -\boldsymbol{I}_{N-1}],
$$

where $\mathcal{T}^o = (\mathcal{V}, \mathcal{E})$ is a directed tree with $|\mathcal{E}| = N-1$ edges that go from every node $j \neq 1$ to the first node. Any other strictly directed tree can be used as in Parada Contzen (2017), but we restrict the analysis to this one for simplicity. With help of this transformation we can define error vectors,

$$
\begin{aligned}
\boldsymbol{e}_p &:= \boldsymbol{T}\bar{\boldsymbol{p}} = \boldsymbol{T}\boldsymbol{F}\boldsymbol{p} \in \mathbb{R}^{N-1} \\
\boldsymbol{e}_q &:= \boldsymbol{T}\bar{\boldsymbol{q}} = \boldsymbol{T}\boldsymbol{F}\boldsymbol{q} \in \mathbb{R}^{N-1},
\end{aligned}
$$

that describes the per unit difference between the power injected at the first node with the power injected in all the other nodes. Note that the error vectors are a reduction of order and therefore there is no inverse function between the normalized powers and their respective errors. However, the following relationship can be stated when considering the properties of the transformation $\boldsymbol{T}$ and its pseudo-inverse $\boldsymbol{T}^+ = \boldsymbol{T}'(\boldsymbol{T}\boldsymbol{T}')^{-1}$:

$$
\begin{aligned}
\boldsymbol{e}_p = \boldsymbol{T}\bar{\boldsymbol{p}} &\iff \bar{\boldsymbol{p}} = \boldsymbol{T}^+\boldsymbol{e}_p + \frac{1}{N}\boldsymbol{1}\boldsymbol{1}'\bar{\boldsymbol{p}} \\
\boldsymbol{e}_q = \boldsymbol{T}\bar{\boldsymbol{q}} &\iff \bar{\boldsymbol{q}} = \boldsymbol{T}^+\boldsymbol{e}_q + \frac{1}{N}\boldsymbol{1}\boldsymbol{1}'\bar{\boldsymbol{q}}.
\end{aligned}
$$

From here, Active Power Sharing can be defined for every $i \neq j \in \mathcal{V}$ as

$$
\lim_{t\to+\infty} P_i/\chi_i = \lim_{t\to+\infty} P_j/\chi_j \iff \lim_{t\to+\infty} \boldsymbol{e}_p = \boldsymbol{0},
$$

and Reactive Power Sharing as

$$
\lim_{t\to+\infty} Q_i/\chi_i = \lim_{t\to+\infty} Q_j/\chi_j \iff \lim_{t\to+\infty} \boldsymbol{e}_q = \boldsymbol{0}.
$$

That is, power sharing is a consensus problem on the elements of the vectors $\bar{\boldsymbol{p}}$ and $\bar{\boldsymbol{q}}$. This is equivalent to a Lyapunov stability problem of the error vectors $\boldsymbol{e}_p$ and $\boldsymbol{e}_q$ as shown in Parada Contzen (2017).

The typical approach to achieve active power sharing is to feedback, through a droop controller or a distributed consensus algorithm, the per unit active power injected by the inverters, in order to modify the operation frequency of the grid. The idea is to temporary delay some voltages to modify the electric angle between them and in that way regulate active power. However, the traditional approach implies that the frequencies at each node vary from its nominal value in stationary state.

Similarly, to achieve reactive power sharing, the feedback of per unit reactive power measurements is done over the amplitude inputs of the inverters, resulting in small variations of the RMS values around the nominal power. Therefore, the synchronization and voltage regulation additional objectives must be considered.

For synchronization, we are interested in the operation frequency of the different inverters connected to the grid to be identical to the nominal value. That is, $\forall i \in \mathcal{V}$, Synchronization is defined as

$$\lim_{t\to+\infty} \omega_{o,i} = \omega \iff \lim_{t\to+\infty} \upsilon_i = \dot{\delta}_i = 0 \iff \lim_{t\to+\infty} \boldsymbol{\upsilon} = \mathbf{0}.$$

This is more restrictive than a simple consensus problem, because we are not interested only in obtaining equal operation frequencies, but we force these frequencies to be equal to the nominal value.

In the case of voltage regulation, the control objective follows a slightly different approach. In opposition to the frequency modification, because the deviation of the voltage amplitudes around the nominal value is necessary for power sharing, we cannot enforce these variations to be zero. However, we can still ask that the mean value of all these deviations is zero so that, in average, all nodes of the grid work at the nominal value. Therefore, we define Voltage Regulation through the following expression:

$$\lim_{t\to+\infty} \bar{\nu} = 0 \iff \lim_{t\to+\infty} \frac{1}{N}\mathbf{1}'\boldsymbol{\nu} = 0.$$

3.2 Proposed Controllers

Based on the control strategies proposed in the already quoted publications, we will consider the controller depicted in Figure 2, which can be described by the following equations:

$$\boldsymbol{u}^{\psi}(t) = \boldsymbol{L}_{pp}\bar{\boldsymbol{p}}(t) + \boldsymbol{L}_{pq}\bar{\boldsymbol{q}}(t) + \boldsymbol{K}_{pp}\int_0^t \boldsymbol{u}^{\psi}(\tau)d\tau \qquad (6)$$

$$\boldsymbol{u}^{V}(t) = \int_0^t \left(\boldsymbol{L}_{pq}\bar{\boldsymbol{p}}(\tau) + \boldsymbol{L}_{qq}\bar{\boldsymbol{q}}(\tau) + \boldsymbol{K}_{qq}\boldsymbol{u}^{V}(\tau)\right)d\tau \qquad (7)$$

The upper branch in the figure is a primary active power sharing controller that modifies the frequency input $\boldsymbol{d}^{\psi} = \omega\mathbf{1} + \boldsymbol{u}^{\psi}$ of the inverters, by an active power feedback through matrix $\boldsymbol{L}_{pp} = -l_{pp}\boldsymbol{I} - \hat{L}(\mathcal{G}_{pp}) \in \mathbb{R}^{N\times N}$, where $l_{pp} \geq 0$ is the droop constant and $\hat{L}(\mathcal{G}_{pp})$ is the Laplacian matrix of a weighted undirected graph $\mathcal{G}_{pp}$ over the set of vertexes $\mathcal{V}$ that compose the microgrid. We also consider a reactive power feedback characterized by matrix $\boldsymbol{L}_{qp} = -l_{qp}\boldsymbol{I} - \hat{L}(\mathcal{G}_{qp}) \in \mathbb{R}^{N\times N}$, with $l_{qp} \geq 0$ and $\mathcal{G}_{qp}$ another weighted graph over the vertexes of the microgrid. An integral secondary controller characterized by $\boldsymbol{K}_{pp} = \mathbf{1}\boldsymbol{k}'_{pp} \in \mathbb{R}^{N\times N}$, with $\boldsymbol{k}_{pp} \in \mathbb{R}^N$, is considered to achieve synchronization.

The lower branch of the controller is associated to the reactive power sharing objective and modify the amplitude input of the inverters $\boldsymbol{d}^{V} = V(\mathbf{1} + \boldsymbol{u}^{V})$. An integral consensus based power feedback is considered to achieve this objective with $\boldsymbol{L}_{qq} = \hat{L}(\mathcal{G}_{qq}) \in \mathbb{R}^{N\times N}$ and $\boldsymbol{L}_{pq} = \hat{L}(\mathcal{G}_{pq})$, where $\mathcal{G}_{qq}$ and $\mathcal{G}_{pq}$ are weighted undirected graphs over $\mathcal{V}$. A secondary controller characterized by $\boldsymbol{K}_{qq} = \boldsymbol{k}_{qq}\frac{1}{N}\mathbf{1}'$, with $\boldsymbol{k}_{qq} \in \mathbb{R}^N$ is also used to achieve voltage regulation.

In the setup from the quoted publications, $\boldsymbol{L}_{pq} = \boldsymbol{L}_{qp} = \mathbf{0}$ because active and reactive power are treated as if they were decoupled. Here we add these matrices in order to have more freedom for tunning the controller to compensate the effect of matrix $\boldsymbol{C}_p$ in model (5). Note that one could further generalize this control strategy by including secondary crossed feedbacks with matrices $\boldsymbol{K}_{qp} \neq \mathbf{0}$ and $\boldsymbol{K}_{pq} \neq \mathbf{0}$ of proper dimensions to force the control input $\boldsymbol{u}^{\psi}$ to depend dynamically on $\boldsymbol{u}^{V}$ and *vice versa*.

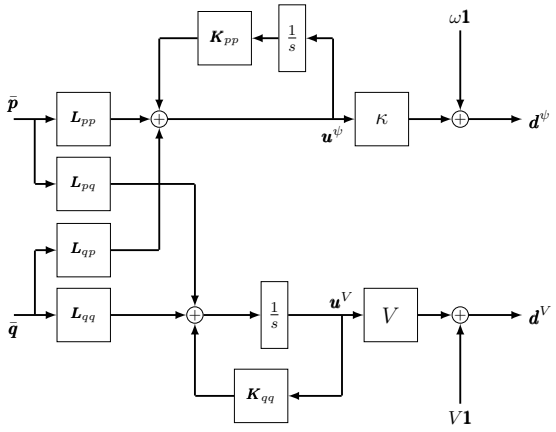

Fig. 2. Control strategy diagram.

Note that the graphs $\mathcal{G}_{pp}$, $\mathcal{G}_{pq}$, $\mathcal{G}_{qp}$, and $\mathcal{G}_{qq}$ might eventually have different sets of edges. However, it is reasonable to define the edges of all graphs identically in order to avoid unnecessary communication efforts. Indeed, if we aim to keep these graphs connected, what is not strictly necessary for the active power branch, we could define the weights of the graphs over a star-tree centered on the i-th node in such a way that only $N-1$ communication links are needed, between the center node and all the others. Additional edges would imply also additional communication links between inverters that are not connected to the i-th node. Furthermore, if the secondary gains are chosen in such a way that $\boldsymbol{k}_{pp} = k_{pp}\boldsymbol{s}_i$ and $\boldsymbol{k}_{qq} = k_{qq}\boldsymbol{s}_i$, with $k_{pp} \in \mathbb{R}$ and $k_{qq} \in \mathbb{R}$, we also restrict the exchange of signals only between the i-th node and the others keeping the needed communication links to a minimum.

3.3 Dynamic behavior of closed loop system

We are interested in finding a dynamical model of the form $\dot{\boldsymbol{x}} = \boldsymbol{A}\boldsymbol{x} + \boldsymbol{B}\boldsymbol{w}$, where $\boldsymbol{x} = \left[\boldsymbol{e}'_p,\ \boldsymbol{e}'_q,\ \boldsymbol{\upsilon}',\ \bar{\nu}\right]$, $\boldsymbol{w} = \left[\bar{\boldsymbol{w}}'_p,\ \bar{\boldsymbol{w}}'_q\right]'$, and matrices $\boldsymbol{A} \in \mathbb{R}^{(3N-1)\times(3N-1)}$ and $\boldsymbol{B} \in \mathbb{R}^{(3N-1)\times(2N)}$ depending on the parameters of the transmission circuit (5) and the described controller.

Note that from the inverse relationships between the errors and the normalized powers we have that

$$\begin{aligned}\boldsymbol{C}_q\boldsymbol{L}_{pp}\bar{\boldsymbol{p}} &= \boldsymbol{C}_q(-l_{pp}\boldsymbol{I} - \hat{L}(\mathcal{G}_{pp}))(\boldsymbol{T}^{+}\boldsymbol{e}_p + \frac{1}{N}\mathbf{1}\mathbf{1}'\bar{\boldsymbol{p}}) \\ &= \boldsymbol{C}_q\boldsymbol{L}_{pp}\boldsymbol{T}^{+}\boldsymbol{e}_p.\end{aligned}$$

Similarly, $\boldsymbol{C}_q\boldsymbol{L}_{qp}\bar{\boldsymbol{q}} = \boldsymbol{C}_q\boldsymbol{L}_{qp}\boldsymbol{T}^{+}\boldsymbol{e}_q$. For the reactive power branch, $\boldsymbol{L}_{qq}\bar{\boldsymbol{q}} = \boldsymbol{L}_{qq}(\boldsymbol{T}^{+}\boldsymbol{e}_q + \frac{1}{N}\mathbf{1}\mathbf{1}'\bar{\boldsymbol{q}}) = \boldsymbol{L}_{qq}\boldsymbol{T}^{+}\boldsymbol{e}_q$ and $\boldsymbol{L}_{pq}\bar{\boldsymbol{p}} = \boldsymbol{L}_{pq}\boldsymbol{T}^{+}\boldsymbol{e}_p$. These expressions can be used to simplify the dynamical equations discussed in the sequel.

For the errors, taking the derivative of model (5), we can write that

$$\begin{bmatrix}\dot{\boldsymbol{e}}_p \\ \dot{\boldsymbol{e}}_q\end{bmatrix} = \begin{bmatrix}\boldsymbol{T}\boldsymbol{F}\boldsymbol{C}_Q & \boldsymbol{T}\boldsymbol{F}\boldsymbol{C}_P \\ -\boldsymbol{T}\boldsymbol{F}\boldsymbol{C}_P & \boldsymbol{T}\boldsymbol{F}\boldsymbol{C}_Q\end{bmatrix}\begin{bmatrix}\dot{\boldsymbol{\delta}} \\ \dot{\boldsymbol{\nu}}\end{bmatrix} + \begin{bmatrix}\boldsymbol{T} & \mathbf{0} \\ \mathbf{0} & \boldsymbol{T}\end{bmatrix}\begin{bmatrix}\bar{\boldsymbol{w}}_p \\ \bar{\boldsymbol{w}}_q\end{bmatrix}.$$

From equation (6) and (4), we have that

$$\dot{\boldsymbol{\delta}} = \kappa \left(\boldsymbol{L}_{pp}\bar{\boldsymbol{p}}(t) + \boldsymbol{L}_{pq}\bar{\boldsymbol{q}}(t) + \boldsymbol{K}_{pp} \int_0^t \boldsymbol{u}^{\psi}(\tau) d\tau \right)$$

Which can be replaced in the expression for the derivative of the errors. Using the inverse relationship between the errors and the powers, and additionally noting that $\boldsymbol{C}_p\boldsymbol{K}_{pp} = \boldsymbol{C}_q\boldsymbol{K}_{pp} = \boldsymbol{0}$, the part of the derivative of the errors that depends on $\dot{\boldsymbol{\delta}}$ can be expressed in terms of the errors only.

For the derivative of the voltage deviations we can derive equation (7) to write, using (4), that

$$\dot{\boldsymbol{\nu}} = \boldsymbol{L}_{pq}\boldsymbol{T}^{+}\boldsymbol{e}_p + \boldsymbol{L}_{qq}\boldsymbol{T}^{+}\boldsymbol{e}_q + \boldsymbol{k}_{qq}\frac{1}{N}\boldsymbol{1}'\boldsymbol{\nu}.$$

Which also depend on the errors and can be replaced in the expressions for the derivative of the errors. As $\bar{\nu} = \frac{1}{N}\boldsymbol{1}'\boldsymbol{\nu}$ and $\boldsymbol{1}'\boldsymbol{L}_{pq} = \boldsymbol{1}'\boldsymbol{L}_{qq} = \boldsymbol{0}$, we obtain immediately from the previous expression that $\dot{\bar{\nu}} = \frac{1}{N}\boldsymbol{1}'\boldsymbol{k}_{qq}\bar{\nu}$. Note that this does not depend on the load or its rate change and that if the control gain were zero, then the mean value of the voltages deviations would remain constant at its initial condition.

Similarly, deriving equation (6) we can obtain an expression for the frequency deviation derivative, $\dot{\boldsymbol{\nu}}$, in terms of the elements of vector $\boldsymbol{x}$. By combining these dynamical expressions with (4), and the inverse relationship between the powers and their respective errors, we can finally write that

$$\frac{d}{dt}\begin{bmatrix}\boldsymbol{e}_p\\ \boldsymbol{e}_q\\ \boldsymbol{\nu}\\ \bar{\nu}\end{bmatrix} = \begin{bmatrix}\boldsymbol{A}_{11} & \boldsymbol{A}_{12} & \boldsymbol{0} & \boldsymbol{A}_{14}\\ \boldsymbol{A}_{21} & \boldsymbol{A}_{22} & \boldsymbol{0} & \boldsymbol{A}_{24}\\ \boldsymbol{A}_{31} & \boldsymbol{A}_{32} & \boldsymbol{A}_{33} & \boldsymbol{A}_{24}\\ \boldsymbol{0} & \boldsymbol{0} & \boldsymbol{0} & \boldsymbol{A}_{44}\end{bmatrix}\begin{bmatrix}\boldsymbol{e}_p\\ \boldsymbol{e}_q\\ \boldsymbol{\nu}\\ \bar{\nu}\end{bmatrix} + \begin{bmatrix}\boldsymbol{T} & \boldsymbol{0}\\ \boldsymbol{0} & \boldsymbol{T}\\ \boldsymbol{B}_{31} & \boldsymbol{B}_{32}\\ \boldsymbol{0} & \boldsymbol{0}\end{bmatrix}\begin{bmatrix}\bar{\boldsymbol{w}}_p\\ \bar{\boldsymbol{w}}_q\end{bmatrix},$$

where

$$\begin{aligned}
\boldsymbol{A}_{11} &= \boldsymbol{T}\boldsymbol{F}\left(\kappa\boldsymbol{C}_q\boldsymbol{L}_{pp} + \boldsymbol{C}_p\boldsymbol{L}_{pq}\right)\boldsymbol{T}^{+},\\
\boldsymbol{A}_{12} &= \boldsymbol{T}\boldsymbol{F}\left(\kappa\boldsymbol{C}_q\boldsymbol{L}_{qp} + \boldsymbol{C}_p\boldsymbol{L}_{qq}\right)\boldsymbol{T}^{+},\\
\boldsymbol{A}_{14} &= \boldsymbol{T}\boldsymbol{F}\boldsymbol{C}_p\boldsymbol{k}_{qq},\\
\boldsymbol{A}_{21} &= \boldsymbol{T}\boldsymbol{F}\left(-\kappa\boldsymbol{C}_p\boldsymbol{L}_{pp} + \boldsymbol{C}_q\boldsymbol{L}_{pq}\right)\boldsymbol{T}^{+},\\
\boldsymbol{A}_{22} &= \boldsymbol{T}\boldsymbol{F}\left(-\kappa\boldsymbol{C}_p\boldsymbol{L}_{qp} + \boldsymbol{C}_q\boldsymbol{L}_{qq}\right)\boldsymbol{T}^{+},\\
\boldsymbol{A}_{24} &= \boldsymbol{T}\boldsymbol{F}\boldsymbol{C}_q\boldsymbol{k}_{qq},\\
\boldsymbol{A}_{31} &= \kappa\left(\boldsymbol{L}_{pp}\boldsymbol{F}\boldsymbol{C}_p + \boldsymbol{L}_{qp}\boldsymbol{F}\boldsymbol{C}_q\right)\boldsymbol{L}_{pq}\boldsymbol{T}^{+},\\
\boldsymbol{A}_{32} &= \kappa\left(\boldsymbol{L}_{pp}\boldsymbol{F}\boldsymbol{C}_p + \boldsymbol{L}_{qp}\boldsymbol{F}\boldsymbol{C}_q\right)\boldsymbol{L}_{qq}\boldsymbol{T}^{+},\\
\boldsymbol{A}_{33} &= \kappa\left(\boldsymbol{L}_{pp}\boldsymbol{F}\boldsymbol{C}_q - \boldsymbol{L}_{qp}\boldsymbol{F}\boldsymbol{C}_p\right) + \boldsymbol{1}\boldsymbol{k}'_{pp},\\
\boldsymbol{A}_{34} &= \kappa\left(\boldsymbol{L}_{pp}\boldsymbol{F}\boldsymbol{C}_p + \boldsymbol{L}_{qp}\boldsymbol{F}\boldsymbol{C}_q\right)\boldsymbol{k}_{qq},
\end{aligned}$$

$\boldsymbol{A}_{44} = \frac{1}{N}\boldsymbol{1}'\boldsymbol{k}_{qq}$, $\boldsymbol{B}_{31} = \kappa\boldsymbol{L}_{pp}$, and $\boldsymbol{B}_{32} = \kappa\boldsymbol{L}_{qp}$.

Note that this closed loop model is not linear with respect to the parameters in matrices $\boldsymbol{L}_{pp}$, $\boldsymbol{L}_{pq}$, $\boldsymbol{L}_{qp}$, and $\boldsymbol{L}_{qq}$. Also, there are several entries that are identically zero. This gives space to define more complex control strategies, for example considering secondary crossed feedback as discussed before.

The dynamic behavior of vector $\boldsymbol{x}$ is not affected directly by the load, but by its change rate, meaning that the control objectives can be achieved for any constant load level, *i.e.* when $\bar{\boldsymbol{w}}_p = \bar{\boldsymbol{w}}_q = \boldsymbol{0}$, if matrix $\boldsymbol{A} \in \mathbb{R}^{(3N-1)\times(3N-1)}$ is Hurwitz. Robustness analysis, for example through $\mathtt{H}_\infty$- or $\mathtt{H}_2$-norms, can also be done to characterize the influence of the change rate of the loads into any of the control objectives.

Table 1. Lines Nominal Parameters.

i	j	$R_{ij}[\Omega]$	$L_{ij}[mH]$
1	2	0.5000	1.1000
1	4	0.9000	1.4000
2	3	0.1000	0.7600
3	4	0.1000	1.5000

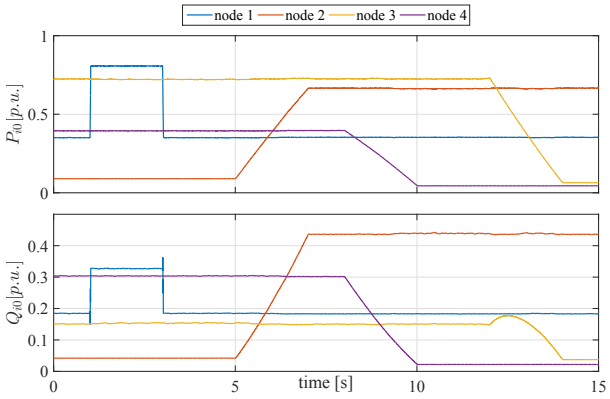

Fig. 3. Load active and reactive powers in per unit, $\bar{\boldsymbol{p}}_0$ and $\bar{\boldsymbol{q}}_0$.

4. NUMERIC EXAMPLE

Consider a microgrid with $N = 4$ nodes, nominal frequency $f = 50[Hz]$, nominal amplitude $V = 220[V_{RMS}]$, and with line parameters described in Table 1. The nominal rating powers, which are also used as per unit bases, are $S_1 = S_2 = 600[VA]$, $S_3 = 300[VA]$, and $S_4 = 500[VA]$ for the respective nodes. The load, non-passive and in per unit, is changing arbitrarily according to the graphs shown in Figure 3.

With $\kappa = 0.01$, we will consider primary control matrices derived from the Laplacian matrix of an undirected star graph $\mathcal{G} = (\mathcal{V}, \{(1,2),(1,3),(1,4)\})$ centered in the first node. With arbitrary droop gains and edges weights, with

$$\hat{L}(\mathcal{G}) = \begin{bmatrix}3 & -1 & -1 & -1\\ -1 & 1 & 0 & 0\\ -1 & 0 & 1 & 0\\ -1 & 0 & 0 & 1\end{bmatrix},$$

we choose

$$\begin{aligned}
\boldsymbol{L}_{pp} &= -3.00\boldsymbol{I} - 0.05\hat{L}(\mathcal{G}), \quad \boldsymbol{L}_{qq} = -0.03\hat{L}(\mathcal{G})\\
\boldsymbol{L}_{qp} &= -0.10\boldsymbol{I} - 0.05\hat{L}(\mathcal{G}), \quad \boldsymbol{L}_{pq} = -0.02\hat{L}(\mathcal{G}).
\end{aligned}$$

Again arbitrarily, for the secondary gains we define,

$$\boldsymbol{k}_{pp} = -175\boldsymbol{s}_1, \qquad \boldsymbol{k}_{qq} = -340\boldsymbol{s}_1.$$

With these matrices, we have that the eigenvalues of matrix $\boldsymbol{A}$ are all real and negative, $\text{eig}\{\boldsymbol{A}\} \in [-175, -12.3708]$. That is, the closed loop microgrid should reach all four control objectives simultaneously. This can be seen in Figure 4, where the per unit injected powers are shown, and Figure 5, where the frequency input and the voltage amplitude deviations are shown.

Note that, as the load is not constant, power sharing and synchronization are not reached instantaneously at every moment. However, the transient behavior of the grid present little differences with the desired situation.

We can characterize the transient behavior of the grid through the corresponding $\mathtt{H}_\infty$-norms of the transfer func-

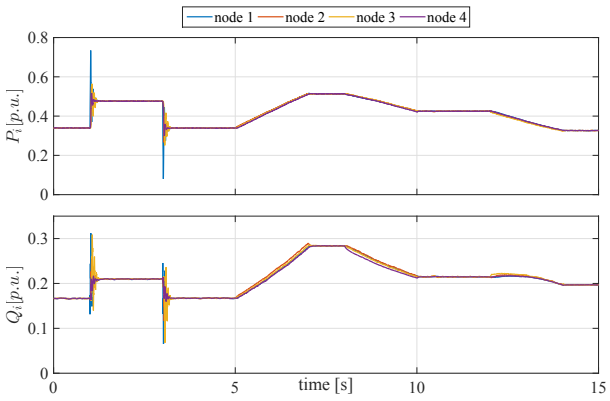

Fig. 4. Generated active and reactive powers in per unit, $\bar{\boldsymbol{p}}$ and $\bar{\boldsymbol{q}}$.

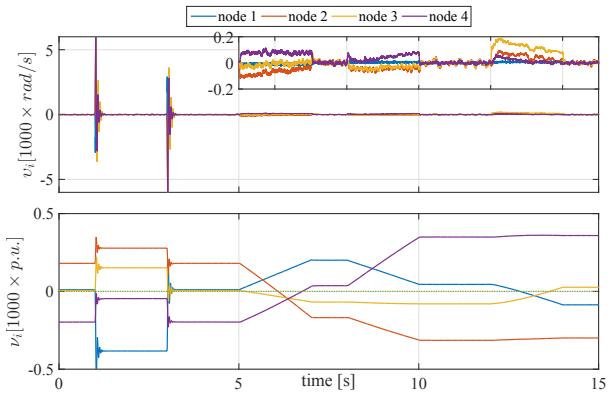

Fig. 5. Frequency input deviation $\boldsymbol{\upsilon}$ (with detail), and voltage amplitude deviation $\boldsymbol{\nu}$.

tions between the change rate of the load powers, $\bar{\boldsymbol{w}} = [\bar{\boldsymbol{w}}_p', \bar{\boldsymbol{w}}_q']'$, to the active power error, the reactive power error, and the frequency deviation, respectively, in this case, $\|H_{\boldsymbol{w},\boldsymbol{e}_p}\|_\infty = 0.0764$, $\|H_{\boldsymbol{w},\boldsymbol{e}_q}\|_\infty = 0.0553$, and $\|H_{\boldsymbol{w},\boldsymbol{\upsilon}}\|_\infty = 0.0023$. As these values are smaller than one, we have that the chosen control strategy attenuates the effect of the load changes on the variables of interest but this effect does not disappear.

5. CONCLUSION

In this paper we dealt with the secondary control of a single phase microgrid considering four control objectives: active and reactive power sharing, frequency restoration, and voltage regulation. The closed loop analysis is performed through a linearized model of the microgrid, where the inverters play the role of control actuators and are controlled in such a way that the four control objectives can be simultaneously reached. The main characteristics of this control strategy are shown within a simulation example.

REFERENCES

Bidram, A. and Davoudi, A. (2012). Hierarchical structure of microgrids control system. *IEEE Transactions on Smart Grid*, 3, 1963– 1976.

Dörfler, F. and Bullo, F. (2013). Kron reduction of graphs with applications to electrical networks. *IEEE Transactions On Circuits and Systems*, 60.

Grainger, J.J. and Stevenson, W.D. (1994). *Power System Analysis*. McGraw-Hill, 1 edition.

Guerrero, J.M., Chandorkar, M., Lee, T.L., and Loh, P.C. (2013). Advanced control architectures for intelligent microgrids, part I. *IEEE Transactions on Industrial Electronics*, 60, 1254–1262.

Guo, F., Wen, C., Mao, J., and Song, Y.D. (2015). Distributed secondary voltage and frequency restoration control of droop-controlled inverter-based microgrids. *IEEE Transactions on Industrial Electronics*, 62.

Guo, F., Wen, C., and Song, Y.D. (2018). *Distributed Control and Optimization Technologies in Smart Grid Systems*. CRC Press.

Han, H., Hou, X., Yang, J., Wu, J., and Guerrero, J.M. (2016). Review of power sharing control strategies for islanding operation of ac microgrids. *IEEE Transactions on Smart Grid*, 7, 200– 215.

Lu, L.Y. and Chu, C.C. (2015). Consensus-based secondary frequency and voltage droop control of virtual synchronous generators for isolated ac micro-grids. *IEEE Journal on Emerging and Selected Topics in Circuits and Systems*, 5, 443– 455.

Palizban, O. and Kauhaniemi, K. (2015). Hierarchical control structure in microgrids with distributed generation: Island and grid-connected mode. *Renewable and Sustainable Energy Reviews*, 44, 797– 813.

Parada Contzen, M. (2017). Consensus in networks with arbitrary time invariant linear agents. *European Journal of Control*, 38, 52– 62.

Parada Contzen, M. (2019). Analysis of consensus in hardware interconnected networks: An application to inverter-based AC microgrids. *European Journal of Control*, 46, 80– 89.

Parada Contzen, M. and Raisch, J. (2016). Reactive power consensus in microgrids. In *European Control Conference (ECC) 2016*.

Peças Lopes, J.A., Moreira, C.L., and Madureira, A.G. (2006). Defining control strategies for microgrids islanded operation. *IEEE Transactions on Power Systems*, 21.

Rocabert, J., Luna, Á., Blaabjerg, F., and Rodríguez, P. (2012). Control of power converters in AC microgrids. *IEEE Transactions on Power Electronics*, 27.

Schiffer, J., Seel, T., Raisch, J., and Sezi, T. (2014). A consensus-based distributed voltage control for reactive power sharing in microgrids. In *13th ECC*.

Schiffer, J., Zonetti, D., Ortega, R., Stanković, A., Sezid, T., and Raisch, J. (2016). A survey on modeling of microgrids—from fundamental physics to phasors and voltage sources. *Automatica*, 74, 135– 150.

Simpson-Porco, J.W., Dörfler, F., and Bullo, F. (2013). Synchronization and power sharing for droop-controlled inverters in islanded microgrids. *Automatica*, 49, 2603– 2611.

Simpson-Porco, J.W., Shafiee, Q., Dörfler, F., Vasquez, J.C., Guerrero, J.M., and Bullo, F. (2015). Secondary frequency and voltage control of islanded microgrids via distributed averaging. *IEEE Transactions on Automatic Control*, 62, 7025– 7038.

Zambroni de Souza, A.C. and Castilla, M. (eds.) (2019). *Microgrids. Design and Implementation*. Springer Nature Switzerland AG, 1 edition.